

Second Order Sliding Mode Observer-Based Control for Uncertain Nonlinear MEMS Optical Switch

H. Fazeli¹ and F. Rahimi²

1. Department of Mechanical Engineering, MalekAshtar University of Technology

2. Aerospace Research Institute

*Tehran, IRAN

hamidfaz2000@yahoo.com

This paper studies the uncertain nonlinear dynamics of a MEMS optical switch addressing electrical, mechanical and optical subsystems. Recently, MEMS optical switch has had significant merits in reliability, control voltage requirements and power consumption. However, an inherent weakness in designing control for such systems is unavailability of switch position information at all times due to the saturated output characteristics, which is aggravated by considering disturbances. In order to circumvent this problem, two nonlinear observers based on the first order and second order sliding mode approach are designed to estimate the state variables of the device subject to external disturbances. The nonlinear observers are then utilized in the control system to maintain robust stability and tracking performances. The newly invented second order sliding mode controller can remove the chattering phenomena as the main drawback of the first order sliding mode controller. Furthermore, since second order sliding mode control is not robust against disturbances/uncertainties which vary with states, a new time-varying second order sliding mode control is proposed to enhance the robust performance of the controller without estimating any switching time. Simulation results show that the proposed observer and control have good tracking ability and robustness against disturbances.

Keywords: Robustness, second order sliding mode observer, second order sliding mode control, MEMS optical switch

Introduction

The main advantage of an optical switch is the conversion of an optical signal to another signal in a direct way. Large scale matrix switches which are mostly used in optical networks now are realized by optical-electronic conversion or electronic switching/electronic-optical conversion. These switches are very expensive and have slow bit rates capacity. To circumvent these problems, the optical switch has been proposed as an obvious solution. Optical switches became important because of the desire in telecommunications industry to focus on all-optical network (AON), which means the total exclusion of electronics.

One approach to optical switching has been the use of MEMS technology to fabricate tiny mirrors that perform the switching function. These tiny mirrors manipulate optical signals directly without converting them to electronic signals. MEMS optical switches are very attractive because of their high capacity, low production cost, compactness, small size and low weight, fast bit rates, low power consumption, integration, and optical transparency [1, 2]. There are numerous applications for optical switches that require precision in positioning of the micro-actuators. For instance, in medical science these devices are capable of concentrating on the particular medical parameters for the purpose of detection and therapy. Recently, advanced space missions are offering high technologies to dramatically enhance the safety and reliability, while reducing the cost of space

1. Assistant Professor (Corresponding Author)
2. PhD Student

transportation. Generally, it costs 25,000 US\$ to put one kilogram of a payload in the Earth orbit. Therefore, MEMS devices are essential for the future space missions. The analog nature of MEMS actuators and their device characteristic uncertainties, due to the manufacturing tolerances, make the implementation of device impractical and/or require costly calibrations. In addition, the nonlinear characteristics of MEMS actuators could result in instability over an extended actuation range in the open-loop operation. This added complexity combined with the submicron precision requirement calls for the development of comprehensive dynamic modeling frameworks along with robust controllers.

Several control strategies have been proposed in the literature for the MEMS optical switch. Owusuet al. [3] designed a controller based on the feedback linearization to compensate the nonlinearity in the system dynamics, and succeeded in stabilizing the switch position of the MEMS optical switch. However, the result was not acceptable by applying the disturbances/uncertainties to the plant. Ebrahimi et al. [4] presented a robust controller based on the traditional sliding mode theory for a MEMS optical switch. Vali et al. [5] introduced the quantitative robust feedback theory to control a nonlinear MEMS optical switch in the presence of parameter variations and unknown disturbances. One of the most important differences between "macro-scale" and "micro-scale" control design is the added modeling uncertainties and nonlinearities in "micro-scale". Hence, the implementation of the proposed controller is attenuated by increasing the inherent complexity of the system.

For the stabilization of an optical switch, it is necessary to dynamically estimate the switch position and velocity. Because, when the switch is near the completely closed or open situation, there is no position information available as a feedback for the control system. Thus, state observers have been introduced to overcome this problem. In [3] a simple nonlinear observer is used to estimate the state variables for a system with Lipschitz nonlinearity in the output characteristics. In this paper, two sliding mode observers are proposed to estimate the state variables for an uncertain nonlinear system. The main advantages of the sliding mode observer are robustness against disturbances/unmodeled dynamics, insensitivity to parameter variations, compact implementation and efficiency for the standard output system.

This paper consists of three major parts. In the first part, two robust sliding mode observers are considered to estimate the switch position and velocity of a MEMS optical switch in the presence of an unknown, but bounded disturbance: 1) first order sliding mode observer (FOSMO) based on the Lyapunov second method [6,7] and 2) second order

sliding mode observer (SOSMO) based on the super-twisting algorithm (STA) [8]. In practice, the second order sliding mode observers are used to estimate the velocity of the system independent of the controller design and they are still successfully implemented to solve the various problems.

In the second part, the estimated state variables are utilized to design the sliding mode controllers. They enable the compact realization of a robust controller, tolerant of device characteristics variations, nonlinearities, and types of inherent instabilities. The main drawback of this approach is the high frequency switching called *chattering*, which can excite the unmodeled high frequency dynamics and make the system unstable [9]. Second order sliding mode control based on STA is one of the recently developed techniques to overcome this difficulty. Here, the discontinuous control acts on the second derivative of the sliding variable instead of the first derivative in the traditional sliding mode control to remove the chattering effect while preserving the advantages of the traditional sliding mode control [10, 11]. Despite the popularity of the STA, it has a major flaw. STA is not robust against disturbances/uncertainties that change with the state variables. One of the methods to enhance the robust performance in the SMC theory is to eliminate the reaching phase using the time-varying sliding mode control (TVSMC) strategy. The concept of TVSMC was introduced by Choi et al. [12] and Bartoszewicz [13]. TVSMC can shorten the reaching phase via a shifting or rotating sliding surface. Yongqian et al. [14] studied the attitude stabilization of a rigid spacecraft based upon the different TVSMCs by designing the switching time between sliding surfaces. In the previous papers, the designed sliding surface included switching time and the designed controller pertained against the initial conditions to shift or rotate the sliding surface. In the present paper, we propose a new TVSMC algorithm without describing the switching time and a designer is able to select both time-varying function and a procedure to shift (known as "intercept-varying") and/or rotate (known as "slope-varying") the sliding surface optionally for every initial conditions. As a result, the main contributions of this paper are to employ:

- Robust observers and controllers simultaneously based on the first- and second-order sliding mode control theories for the MEMS optical switch. These devices can be used in space missions (e.g. remote sensing and communication satellites) because of the presence of high resolution and reliability, and minimum weight, size and power consumption.
- Time-varying sliding mode control technique to enhance the robustness of the second-order sliding mode in the presence of parameter uncertainty. The proposed TVSMC does not need any switching time between sliding surfaces and it can be applied to the various SMC strategies with any initial conditions.

Mathematical Model

A general optical switch structure consisting of an electrostatic comb drive, the body of the device, and a blade or shuttle is shown in Fig.1. The voltage applied to the comb drive actuator generates a force that moves the shuttle attached micro-mirror that cuts a light beam exiting a transmitting fiber and being collected in a receiving and modulating density.

In order to derive a mathematical model of system dynamics it is needed to determine parameters of the relevant differential equation that describes forces acting on the shuttle. It is assumed that the shuttle has one degree of freedom and moves only in one direction. It is important to mention that there might be other degrees of freedom, like rotation around the main body axes, translation along them, as well as different vibrational modes. However, only the main degree of freedom will be considered in this paper and also the related materials for modeling purpose are referred to [15].

The mathematical model of the switch has three main components: an electrical, a mechanical and an optical component. Altogether, the system can be described with a second order nonlinear differential equation as:

$$m\ddot{x} + d(x, \dot{x}) + k(x) = f(V, x) \tag{1}$$

$$P = h(x) \tag{1}$$

where m is the effective moving mass of the shuttle, d is a function describing losses such as damping and friction, k is the stiffness of the suspension, f is the electrostatic force acting on the model, P is light intensity and x is the shuttle position.

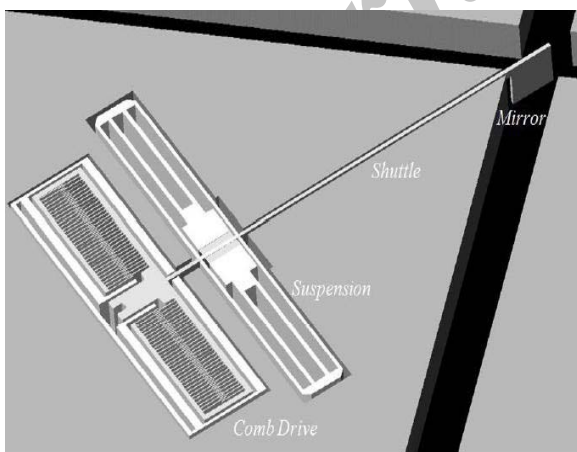


Figure 1. Image of a MEMS optical switch

The system exact parameters m , d , k and f are not easy to obtain and we will go step by step to determine all of these parameters. First, the electrical model is built and then the optical model connects the position of the shuttle to the intensity of the sensed light.

Electrical Model

The electrical part of the model considers generation of the induced electrostatic force by applying voltage to the actuator. The capacitance of the comb drive as a function of position should be determined first. Capacitance of the comb drive can be calculated as the sum of all of parallel capacitances among pairs of comb electrodes. The total capacitance is given as a function of position by[15]:

$$C(x) = \frac{\epsilon_0 A}{d_G} = \frac{2n\epsilon_0 T(x+x_0)}{d_G} \tag{2}$$

where $\epsilon_0 = 8.854 \times 10^{-12} Fm^{-1}$ is the dielectric constant of vacuum, n is the number of the movable comb fingers ($n=150$), T is thickness of the structural layer ($T = 35\mu m$), d_G is the length of the gap between fingers ($d_G = 2.6\mu m$) and x_0 is the overlapped length of fingers when no voltage is applied ($x_0 = 15\mu m$). At rest position, the capacitance of the comb drive is about $0.27pF$ when $x = 0$ and $x = 15\mu m$, which increases as force is applied and the fingers move closer. Generally, the electrostatic force of the capacitor is given as the product of squared voltage and change of capacitance with respect to position as:

$$f(V, x) = \frac{1}{2} V^2 \frac{\partial C}{\partial x} \tag{3}$$

where V is the voltage applied over the electrodes. By combining (2) and (3) electrostatic force can be calculated as:

$$f(V, x) = \frac{n\epsilon_0 T}{d_G} V^2 = k_e V^2 \tag{4}$$

where k_e is defined as the input gain of the system with the value of $k_e = 17.8 nN/V^2$.

It is interesting to note that capacitance (2) depends linearly on position over a wide range of deflections. It is one of the most important characteristics of the comb drive. Generally, for other configurations, this is not the case and capacitance is a higher nonlinear function of position x . It should be noted that the linear relationship does not hold for extreme deflections and may cause considerable undesired results that necessitate using a robust control scheme to meet such uncertainties.

Mechanical Model

In order to obtain the mechanical model of the system, three parameters namely, the effective moving mass m , the damping coefficient d and stiffness of the suspension k have to be determined. Effective mass for the switch can be expressed as [15]

$$m = m_{mirror} + \frac{1}{2} m_{rigid} + 2.74 m_{beam} \tag{5}$$

when calculated, the effective mass of the system is $m = 2.39 \times 10^{-9} kg$.

Stiffness is generally a nonlinear function of position $f=k(x)$. For most metals and for silicon spring-like structures, it can be described as $k(x) = k_x x + k_{x3} x^3$. For the suspension given in this paper, stiffness of the beam is assumed to be a linear function of the position and its coefficient is given as $k_x = k = 0.46 \text{ N/m}$.

Damping, or energy dissipation, is the most difficult parameter to be determined analytically, despite using FEA. The reason lies in the number of different mechanisms that cause it including friction, viscous forces, drag, etc. We will consider viscous forces as the primary causes of damping. Four different mechanisms contribute to damping, Couette flow, Poiseuille flow, Stokes flow, and Squeeze film damping [16]. Generally, they can be summarized as $f_d = (d_x x + d_0) \dot{x}$. When actual parameters are substituted, damping is expressed as [17]:

$$d(x, \dot{x}) = 0.0363(x + 15 \times 10^{-6}) \dot{x} \quad (6)$$

Optical Model

The optical model is simply a function that connects the intensity of light to the position of the blade as in Fig.2. Light beam is intercepted by the blade, increasing and decreasing the throughput of light. The Rayleigh-Somerfield model is based on a Gaussian distribution of the intensity across the light beam.

Transmitted power can be described as [17]:

$$= \frac{1}{2} \left[1 - \text{Erf} \left(\frac{\sqrt{2}(x-\eta_0)}{w_1} \right) \right] \quad (7)$$

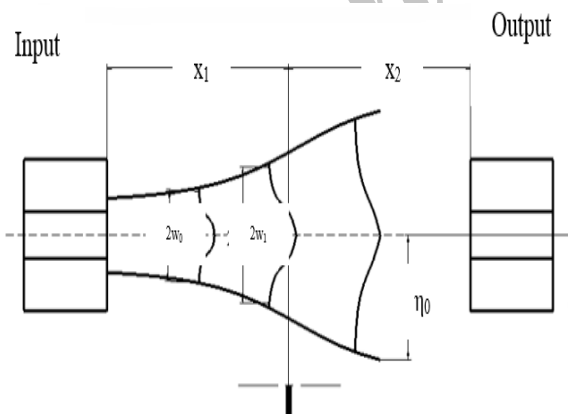


Figure 2. Optical Model

wherew₁ = 10.9 μm and η₀ = 11.2 μm.

The relationship between the power ratio and the position of the mirror is shown in Fig.3. It is important to note that the attenuation curve is saturated by the error function which makes it difficult to reconstruct the states in saturation region for control design purposes.

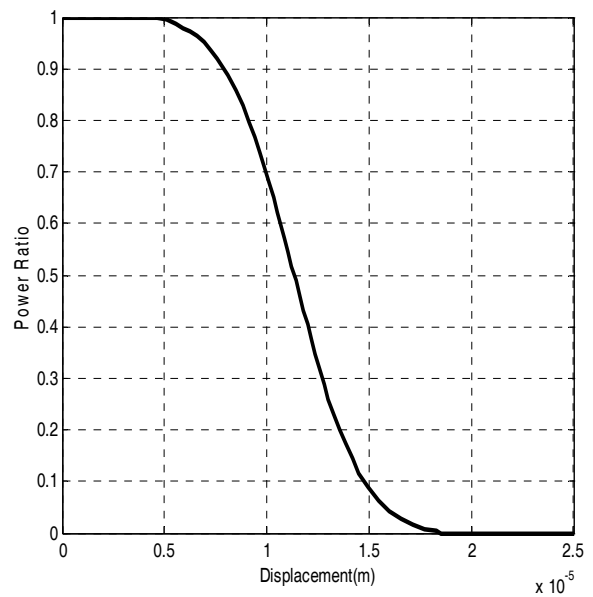


Figure 3. Power ratio against displacement

Consequently, integrating the created models for each section and applying the procedures done for increasing accuracy of the model in [2], result in the nonlinear mathematical model of the switch as:

$$\ddot{x} = \frac{1}{2.35 \times 10^{-9}} [-(0.0363x + 4.5 \times 10^{-3}) \dot{x} - 0.6x + 1.9 \times 10^{-8} V^2 + \xi(t, x, \dot{x}, V)] \quad (8)$$

where V^2 (quadric term in voltage) is the input and ξ represents the uncertainties affecting the MEMS optical switch which is assumed to be bounded to a positive known term $\eta(t, x, \dot{x})$. As mentioned above, these uncertainties mostly come from simplifications in electrical and mechanical model of device.

Design of Sliding Mode Observers

Sliding mode observers are very useful means which have been developed for many reasons like working with reduced observation error dynamics, possibility of obtaining a step by step design, a finite time convergence for all the observable states and robustness against uncertainties [6].

At first, a traditional first order sliding mode observer (FOSMO) is proposed. The well-known problems when using the FOSMOs are the relative degree one requirement and the chattering phenomena. In order to deal with these limitations while preserving the main advantages of the FOSMOs such as finite-time convergence and robustness against disturbances, second order sliding mode observers (SOSMO) are proposed for system state observation. This kind of observer does not require the relative degree of the sliding manifold to be one, and can totally remove the chattering effect [8].

First Order Sliding Mode Observer (FOSMO) Design

The state space representation of (8) can be rewritten as:

$$\begin{aligned} \dot{x}_1 &= x_2 \\ \dot{x}_2 &= -\frac{k}{m}x_1 - \frac{1}{m}(d_1x_1 + d_0)x_2 \\ &\quad + \frac{k_e}{m}V^2 + \xi(t, x_1, x_2, V) \end{aligned} \tag{9}$$

$$y = x_1$$

where $x = [x_1 \ x_2]^T$, and x_1, x_2 denote the switch position and velocity, respectively.

Lets consider a traditional sliding mode observer for the MEMS optical switch (9) as [6]:

$$\begin{aligned} \dot{\hat{x}}_1 &= \hat{x}_2 + \lambda_1 \text{sign}(x_1 - \hat{x}_1) \\ \dot{\hat{x}}_2 &= -\frac{k}{m}x_1 \\ &\quad - \frac{1}{m}(d_1x_1 + d_0)(\hat{x}_2 + \lambda_1 \text{sign}(x_1 - \hat{x}_1)) \\ &\quad + \frac{k_e}{m}V^2 + \lambda_2 \text{sign}(\lambda_1 \text{sign}(x_1 - \hat{x}_1)) \end{aligned} \tag{10}$$

By taking $e = x - \hat{x}$, the error observation dynamics are obtained from (9) and (10) as:

$$\begin{aligned} \dot{e}_1 &= e_2 - \lambda_1 \text{sign}(e_1) \\ \dot{e}_2 &= -\frac{1}{m}(d_1x_1 + d_0)(e_2 - \lambda_1 \text{sign}(e_1)) \\ &\quad + \xi(t, x_1, x_2, V) - \lambda_2 \text{sign}(\lambda_1 \text{sign}(e_1)) \end{aligned} \tag{11}$$

Now, let us consider the nonempty manifold $s_1 = \{e_1/e_2 = 0\}$ in which the attractivity of s_1 is proved by using the second method of Lyapunov. Let the Lyapunov function be $V_1 = \frac{1}{2}e_1^2$. Differentiating V_1 with respect to time results in:

$$\begin{aligned} \dot{V}_1 &= \dot{e}_1 e_1 \\ &= e_1(e_2 - \lambda_1 \text{sign}(e_1)) \end{aligned} \tag{12}$$

Obviously, if λ_1 is chosen sothat $\lambda_1 > |e_2|_{max}$, then $\dot{V}_1 < 0$ is sufficiently ensured. It means that by decreasing the Lyapunov function with respect to time, the convergence to the sliding surface $s_1 = 0$ will be obtained in finite time t_1 . In other words, for $\lambda_1 > |e_2|_{max}$, \hat{x}_1 converges to x_1 in finite time and remains equal to x_1 for $t > t_1$. Moreover, for $t > t_1$, $\dot{e}_1 \approx 0$, so that from (11)

$$e_2 = \lambda_1 \text{sign}(e_1) \tag{13}$$

After time t_1 , the observantion error dynamics are now equal to

$$\begin{aligned} \dot{e}_1 &= 0 \\ \dot{e}_2 &= \xi(t, x_1, x_2, V) - \lambda_2 \text{sign}(e_2) \end{aligned} \tag{14}$$

By setting $V_2 = \frac{1}{2}(e_2^2 + e_2^2)$,

$$\begin{aligned} \dot{V}_2 &= e_1 \dot{e}_1 + e_2 \dot{e}_2 \\ &= e_2(\xi(t, x_1, x_2, V) - \lambda_2 \text{sign}(e_2)) \end{aligned} \tag{15}$$

Consequently, e_2 goes to zero in finite time $t_2 > t_1$ if $\lambda_2 > \eta(t, x, \dot{x})$. In practice, the signum function $\text{sign}(e)$ can be replaced by a continuous function $\frac{e}{|e|+\gamma}$ to alleviate chattering, where γ is a positive scalar constant.

Second Order Sliding Mode Observer (SOSMO) Design

In order to estimate the state variables of the MEMS optical switch without chattering effect, the following second order sliding mode observer is designed as [8]

$$\begin{aligned} \dot{\hat{x}}_1 &= \hat{x}_2 + \beta |x_1 - \hat{x}_1|^{1/2} \text{sign}(x_1 - \hat{x}_1) \\ \dot{\hat{x}}_2 &= -\frac{k}{m}x_1 - \frac{1}{m}(d_1x_1 + d_0)\hat{x}_2 \\ &\quad + \frac{k_e}{m}V^2 + \alpha \text{sign}(x_1 - \hat{x}_1) \end{aligned} \tag{16}$$

where \hat{x} represents the observed state and α, β are the second order sliding mode observer gains. It is important to note that the initial moment $\hat{x}_1(0) = x_1(0)$ and $\hat{x}_2(0) = 0$ are taken to ensure the observer convergence.

By taking $e = x - \hat{x}$, the error observation dynamics are obtained from (9) and (16) as:

$$\begin{aligned} \dot{e}_1 &= e_2 - \beta |e_1|^{1/2} \text{sign}(e_1) \\ \dot{e}_2 &= -\frac{1}{m}(d_1x_1 + d_0)e_2 + \xi(t, x_1, x_2, V) \\ &\quad - \alpha \text{sign}(e_1) \end{aligned} \tag{17}$$

In our case, the system states are bounded, then the existence is ensured of a constant f^+ , sothat the inequality

$$\left| \xi(t, x_1, x_2, V) - \frac{1}{m}(d_1x_1 + d_0)e_2 \right| < f^+ \tag{18}$$

holds for any possible t, x_1, x_2 and $|\hat{x}_2| \leq 2v_{max} \cdot v_{max}$ and x_{max} are defined sothat $\forall t \in \mathbb{R}^+, \exists x_1, x_2: |x_1| \leq x_{max}, |x_2| \leq v_{max}$. The state boundedness is true, sincethe control input V is bounded ($0 < V < 35 \text{ Volt}$) based on the system hardware [18]. Consequently, the system (8) is bounded input bounded state stable, because for each initial state and each bounded input, the corresponding solution is bounded for $t > 0$. Therefore, f^+ can be written as:

$$f^+ = \frac{3}{m}(d_1x_{max} + d_0)v_{max} + \eta \tag{19}$$

Let α and β satisfy the following inequalities:

$$\begin{aligned} \alpha &> f^+ \\ \beta &> \sqrt{\frac{2}{\alpha - f^+} \frac{(\alpha + f^+)(1 + p)}{1 - p}} \end{aligned} \tag{20}$$

where ρ is some chosen constant, $0 < \rho < 1$.

Theorem1: Suppose that the parameters of the observer (16) are selected according to (20), and condition (18) holds for system (9). Then, the variables of the proposed second order sliding mode observer (16) converge in finite time to the state variables of system (9), i.e., $(\hat{x}_1, \hat{x}_2) \rightarrow (x_1, x_2)$.

Proof. The proof was given by Davila and Fridman in [8].

Sliding Mode Control Design

In this section, the sliding mode theory is employed to control the switch position of a MEMS optical switch. By ensuring that the sliding mode observation is obtained in the previous section, a particular type of variable structure controller (VSC) scheme is presented to combine the controller and observer.

At first, a traditional first order sliding mode controller (FOSMC) is proposed for the nonlinear uncertain system. Based on the traditional sliding mode theory, the system state satisfies the dynamic equation that governs the sliding mode all the time. This requires infinite switching that causes chattering as a main drawback of this approach as it may excite unmodeled high frequency dynamics of the system[9]. The second order sliding mode control (SOSMC) scheme is one of the recently developed techniques which can overcome this difficulty. Here, the discontinuous control acts on the 2nd derivative of sliding variable instead of the first derivative in the traditional sliding mode. This group of controllers does not require the relative degree to the sliding manifold to be one, and can totally remove chattering effect and preserve the main advantages of the traditional sliding mode such as finite time convergence and robustness against uncertainties.

In each part of the control design processes, i.e. FOSMC and SOSMC, at first, we assume that the actual switch position and velocity are available. It helps to investigate the effects of using the observed state variables, rather than actual state variables, on the characteristic response of the closed-loop system. Then, two different controls are presented by using the estimated state variables which are obtained by the designed nonlinear observers in the previous section due to the unavailability of the state variables for measurement in practice.

First Order Sliding Mode Control (FOSMC) Design

In the first case, to design the robust sliding mode control, the sliding surface ($s = 0$) is considered using actual states from (9) with observability assumption of the system. This expression can be written in the form of

$$s = x_2 - \dot{x}_d + \lambda(x_1 - x_d) = 0 \quad (21)$$

To ensure that the actual states of the system approach the sliding mode, $\dot{s} = 0$ should be satisfied. Substitution of the actual states from (9), results in the following expression for equivalent control, U_{eq} .

$$U_{eq} = \frac{1}{k_e} \{kx_1 + (d_x x_1 + d_0)x_2 + m[\ddot{x}_d - \lambda(x_2 - \dot{x}_d)]\} \quad (22)$$

Finally, the sliding mode control law (input voltage) with availability of the system states assumption will be as:

$$V^2 = U_{eq} - \frac{m}{k_e} \rho \text{sign}(s) \quad (23)$$

where ρ is a constant parameter depending on the disturbance exerted on the system and reaching time. By using the second method of Lyapunov, let the Lyapunov function be $V = \frac{1}{2}s^2$. Differentiating V with respect to time results in

$$\begin{aligned} \dot{V} &= s\dot{s} \\ &= s(-\rho \text{sign}(s) + d(t)) \\ &\leq s(-\rho \text{sign}(s) + d_{max}) \end{aligned} \quad (24)$$

Obviously, if $\rho \geq d_{max}$ is satisfied, then $\dot{V} < 0$ is sufficiently ensured.

In the second case, to design sliding mode observer-controller, the sliding surface ($\hat{s} = 0$) is considered using the estimated states from traditional FOSMO dynamics (10) and/or SOSMO dynamics (16). This expression can be written in the form of

$$\hat{s} = \hat{x}_2 - \dot{x}_d + \lambda(\hat{x}_1 - x_d) = 0 \quad (25)$$

Also, to ensure that the estimated states of the system approach the sliding mode, $\dot{\hat{s}} = 0$ should be satisfied. Substitution of the estimated states from traditional FOSMO (10), results in the following expression for equivalent control, \hat{U}_{eq1} .

$$\begin{aligned} \hat{U}_{eq1} &= \frac{1}{k_e} \{kx_1 + (d_1 x_1 + d_0)(\hat{x}_2 + \lambda_1 \text{sign}(x_1 - \hat{x}_1)) \\ &\quad - m\lambda_2 \text{sign}(\lambda_1 \text{sign}(x_1 - \hat{x}_1)) \\ &\quad + m[\ddot{x}_d - \lambda(\hat{x}_2 + \lambda_1 \text{sign}(x_1 - \hat{x}_1) - \dot{x}_d)]\} \end{aligned} \quad (26)$$

On the other hand, substitution of the estimated states from SOSMO (16), results in the following expression for equivalent control, \hat{U}_{eq2} .

$$\begin{aligned} \hat{U}_{eq2} &= \frac{1}{k_e} \{kx_1 + (d_1 x_1 + d_0) \\ &\quad - m\alpha \text{sign}(x_1 - \hat{x}_1) \end{aligned} \quad (27)$$

$$+m[\ddot{x}_d - \lambda(\hat{x}_2 + \beta|x_1 - \hat{x}_1|^{1/2}\text{sign}(x_1 - \hat{x}_1) - \dot{x}_d)]\}$$

Finally, the sliding mode controller will be as:

$$\hat{V}^2 = \hat{U}_{eq} - \frac{m}{k_e} \hat{\rho} \text{sign}(\hat{s}) \tag{28}$$

where $\hat{\rho}$ is a constant parameter just depending on the reaching time. It is important to note that by using real states from (9), ρ is a constant parameter depending on the unknown bounded disturbance exerted on the system and reaching time. By using the second method of Lyapunov, let the Lyapunov function be $V = \frac{1}{2} \hat{s}^2$.

$$\begin{aligned} \dot{V} &= \hat{s} \dot{\hat{s}} \tag{29} \\ &= \hat{s}(-\rho \text{sign}(\hat{s})) \\ &= -\rho |\hat{s}| \end{aligned}$$

Obviously, if $\hat{\rho} > 0$, then $\dot{V} < 0$ is sufficiently ensured.

Second Order Sliding Mode Control (SOSMC) Design

Traditional sliding mode control is obtained by constraining the sliding variable s to zero by discontinuous control acting on the first derivative of the sliding variable. The discontinuous control law is applied only when the sliding variable s has a relative degree one with respect to the control input. If the relative degree is two or more, then a higher order sliding mode (HOSM) can be applied for the control purpose [10]. Here, we will concentrate only on the second order sliding mode control scheme.

Consider an uncertain single-input nonlinear system whose dynamics can be defined by the differential equation

$$\dot{x}(t) = f(t, x(t), u(t)) \tag{30}$$

where $x \in \mathbb{R}^n$ is the state vector, $u \in \mathbb{R}$ is the bounded input, t is the independent variable time, and $f: \mathbb{R}^{n+2} \rightarrow \mathbb{R}^n$ is a sufficiently smooth uncertain vector function. The control task is to accomplish the state trajectory on a proper sliding manifold defined by $s(t) = s(t, x(t)) = 0$

where: $\mathbb{R}^{n+1} \rightarrow \mathbb{R}$ is a known single valued function so that its total time derivatives $s^{(k)}, k = 0, 1, \dots, r - 1$ along the system trajectories exist and are single valued functions of the system state x . It means that discontinuity does not appear in the first $r - 1$ total time derivatives of the sliding variable s .

By differentiating the sliding variable s twice, the following relationships are derived:

$$\dot{s}(t) = \dot{s}(t, x(t), u(t)) \tag{32}$$

$$= \frac{\partial}{\partial t} s(t, x) + \frac{\partial}{\partial x} s(t, x) \cdot f(t, x, u)$$

$$\begin{aligned} \ddot{s}(t) &= \ddot{s}(t, x(t), u(t), \dot{u}(t)) \\ &= \frac{\partial}{\partial t} \dot{s}(t, x, u) + \frac{\partial}{\partial x} \dot{s}(t, x, u) \cdot f(t, x, u) \\ &\quad + \frac{\partial}{\partial u} \dot{s}(t, x, u) u(t) \end{aligned} \tag{33}$$

Depending on the relative degree with respect to control input of the nonlinear SISO system (30), (31), different cases should be considered:

- 1) relative degree $p = 1$, i.e., $\frac{\partial}{\partial u} \dot{s} \neq 0$
- 2) relative degree $p = 2$, i.e., $\frac{\partial}{\partial u} \dot{s} = 0, \frac{\partial}{\partial u} \ddot{s} \neq 0$

In case 1, the traditional sliding mode control solves the problem, but here second order sliding mode control can be used to avoid the chattering effect. In this case, the time derivative of control input $\dot{u}(t)$ appears in the second derivative of sliding variable. By applying $\dot{u}(t)$ as the actual control variable, the chattering is avoided as $\dot{u}(t)$ is discontinuous so the plant control $u(t)$ is continuous. $u(t)$ can be considered as the continuous output of a first order dynamic system that is driven by a discontinuous signal which may be inherently present in the system (fast actuators) or externally introduced. So when the second order sliding mode control approach is applied to the system with relative degree 1, discontinuous $\dot{u}(t)$ steers both s and \dot{s} to zero [10]. In case 2, problem arises when the output control problem of the system with relative degree 2 is faced or when the differentiation of a smooth signal is considered [10].

In order to define the control problem based on second order sliding mode the following conditions must be assumed:

- The control values belong to the closed set $U = \{u: |u| \leq u_m\}$, where u_m is a real constant.
- There exists $u_1 \in (0, 1)$, so that for any continuous function $u(t)$ with $|u(t)| > u_1$, there is t_1 , so that $s(t)u(t) > 0$ for each $t > t_1$. Hence, the control $u(t) = -\text{sign}(s(t_0))$, where t_0 is the initial value of time and provides hitting of the surface $s = 0$ in finite time.
- Given \dot{s} , the total time derivative of the sliding variable s , there are positive constants $s_0, u_0 < 1, \Gamma_m, \Gamma_M$, so that if $|s| < s_0$, then

$$0 < \Gamma_m \leq \frac{\partial}{\partial u} \dot{s}(t, x, u) \leq \Gamma_M \tag{34}$$

For the MEMS optical switch such bounds were obtained from a detailed analysis of the system structure together with comprehensive simulation studies, using a stabilizing control that maintains the system in a secure operation region. As a result, the following bounds were determined as below:

$$\Gamma_m = 0.9 \quad \Gamma_M = 20$$

- There is a positive holds

$$\left| \frac{\partial}{\partial t} \dot{s}(t, x, u) + \frac{\partial}{\partial x} \dot{s}(t, x, u) f(t, x, u) \right| \leq \varphi \tag{35}$$

where for the MEMS optical switch, this bound was determined as $\varphi = 7.6 \times 10^{10}$.

For $|s| < s_0$, the following inequality is defined by the following control law which is given as sum of two components and the corresponding sufficient conditions for the finite time convergence to the sliding manifold are [11]:

$$\begin{aligned} u(t) &= u_1(t) + u_2(t) \\ \dot{u}_1(t) &= -W \text{sign}(s) \\ u_2(t) &= \begin{cases} -\gamma |s_0|^p \text{sign}(s) & \text{if } |s| > |s_0| \\ -\gamma |s|^p \text{sign}(s) & \text{if } |s| \leq |s_0| \end{cases} \end{aligned} \quad (36)$$

$$\begin{aligned} W &> \frac{\varphi}{\Gamma_m} \\ \gamma^2 &\geq \frac{4\varphi}{\Gamma_m^2} \frac{\Gamma_m(W+\varphi)}{\Gamma_m(W-\varphi)} \\ 0 &< p \leq 0.5 \end{aligned} \quad (37)$$

Note that the above algorithm does not require measurements of the time derivative of the sliding variable (\dot{s}), thus, this controller is obviously robust with respect to measurement noises.

Proposed Time-Varying Sliding Mode Control (TVSMC) Design

The phase trajectory of the SMC is divided in two phases: reaching phase and sliding phase. In the reaching phase, the system trajectory starts from a given initial condition and reach the sliding surface. In the sliding phase, the system trajectory lies on the predetermined sliding surface and converges to the desired condition. The motion of the control system in the reaching phase is sensitive to external disturbances and parameter variations, while the system trajectory is insensitive to disturbances/uncertainties during sliding phase. There fore, one of the methods to increase the robust performance of the SMC technique is to shorten the reaching phase. Eventually, the following sliding surface is suggested:

$$\sigma = \dot{e} + H(-e\dot{e})g(t)\lambda e + H(e\dot{e})(\lambda e + h(t)) \quad (38)$$

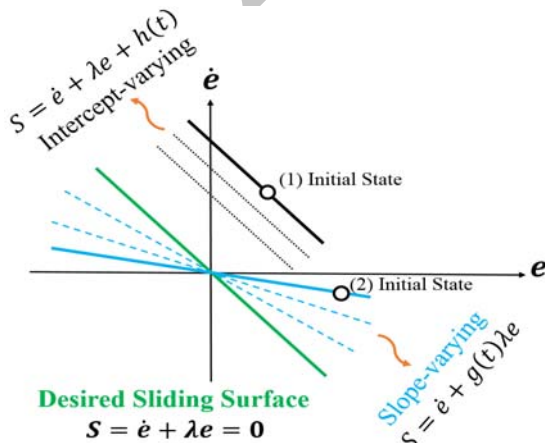


Figure 4. Time-varying sliding surfaces based on the initial condition

where σ is a proposed sliding surface, e is the state error, $g(t)$ and $h(t)$ are two nonlinear time-varying functions. $H(x)$ is a heaviside step function which can be obtained by the Dirac delta function (δ) as:

$$H(x) = \int_{-\infty}^x \delta(t) dt \quad (39)$$

Figure 4 schematically describes a procedure whereby the proposed sliding surface varies over time based on the initial conditions and consequently converges to the desired sliding surface (green line). This procedure suggests that when $e\dot{e} > 0$, the intercept-varying methodology is selected until $e\dot{e} \leq 0$, in which the slope-varying methodology can be used. Therefore, one can easily conclude that there is no switching time between the designed time-varying surfaces.

Next, the design procedure of the proposed two nonlinear functions is studied. First, the initial values for $g(t)$ and $h(t)$ functions must be defined so that the initial states lie on the sliding surface i.e.,

$$\begin{aligned} \dot{e}(0) + g(0)\lambda e(0) &= 0 \Rightarrow g(0) = -\frac{\dot{e}(0)}{\lambda e(0)} \\ \dot{e}(0) + \lambda e(0) + h(0) &= 0 \Rightarrow \\ h(0) &= -(\dot{e}(0) + \lambda e(0)) \end{aligned} \quad (40)$$

There after, functions $g(t)$ and $h(t)$ should be selected so that the slope-varying and/or intercept-varying sliding surfaces approach the desired sliding surface when time tends to infinity. As an example, one may choose the following nonlinear functions:

$$\begin{aligned} g(t) &= g(0) + (1 - g(0)) \tanh t \\ h(t) &= h(0)(1 - \tanh t) \end{aligned} \quad (41)$$

Simulation Results

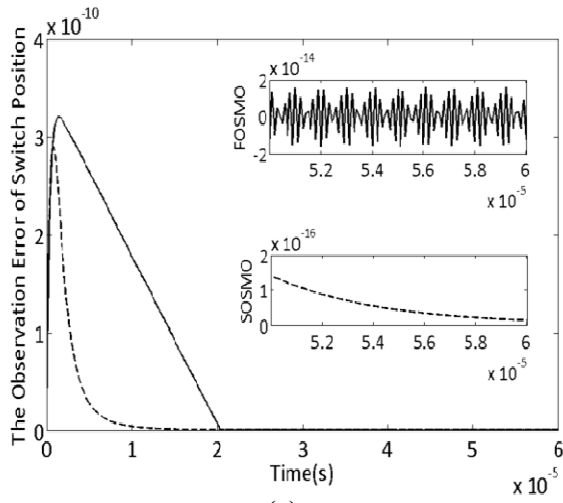
At first, the performances of the proposed nonlinear observers (10) and (16) for estimation of the state variables, are simulated on the MEMS optical switch with the following initial conditions $\mathbf{x}_0 = [10^{-6} \ 10^{-6}]^T$ and $\hat{\mathbf{x}}_0 = [0 \ 0]^T$. Moreover, we consider an unknown disturbance exerted on the system as $d(t) = D \sin \omega t$, where $D = 10^{-6}$ and $\omega = \pi$. The observation gains λ_1, λ_2 for FOSMO (10) and the observation gains α, β for SOSMO (16) are chosen according to Table 1.

Table 1. Sliding mode observer parameters

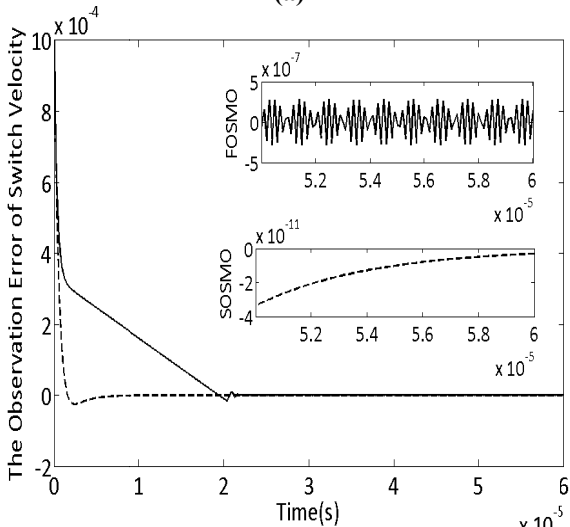
FOSMO	SOSMO
$\lambda_1 = 0.1$	$\alpha = 40000$
$\lambda_2 = 50$	$\beta = 4000$

Figures 5a and 5b show that the second order sliding mode observation error of switch position and switch velocity quickly converge to zero in comparison with the conventional first order sliding mode observation error. Moreover, it is obvious that

the chattering effect has been totally removed through the second order sliding mode observation.



(a)



(b)

Figure 5. a) Observation errors of switch position, b) Observation errors of switch velocity

Table 2. Sliding mode controller parameters

FOSMC	SOSMC
	$W = 5 \times 10^8$
$\rho = 5 \times 10^{-6}$	$\gamma = 10000$
	$p = 0.5$

In the next step, the performances of the proposed control schemes are demonstrated. The desired positions are $x_d = 5\mu m$ and $23\mu m$. The parameters of the proposed controllers are chosen according to Table 2. It is important to recall that the sliding variable is taken as the same in both procedures. According to (21) and (25), $s = 0$ is a line in the phase plane of slope λ and containing the point $x_d = [x_d \ \dot{x}_d]^T$. In our study, $\lambda = 2$ is chosen.

The closed-loop response, control input (applied voltage), phase plane, and sliding variable of the system for short ($5\mu m$) and long ($23\mu m$) displacement of actuator by using classic sliding mode control scheme,

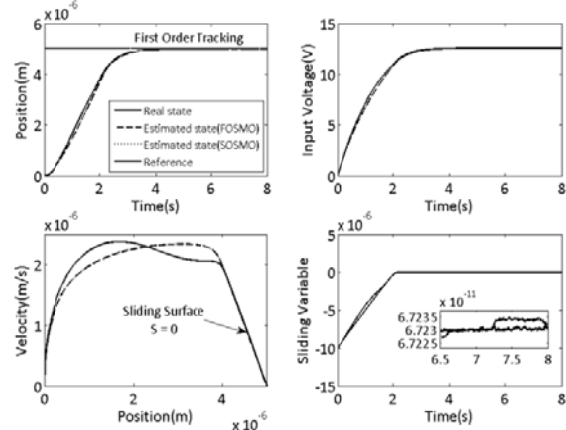


Figure 6. Position, Control input, Phase Plane, and Sliding variable of the system for a short desired position $x_d = 5\mu m$ by using FOSMC

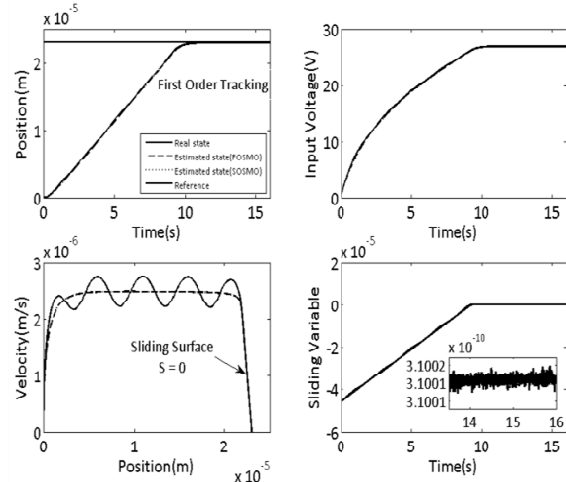


Figure 7. Position, Control input, Phase plane, and Sliding variable of the system for a long desired position $x_d = 23\mu m$ by using FOSMC

are shown in Figs.6 and 7 and by using the second order sliding mode control scheme, are shown in Figs.8 and 9. Moreover, the results of the proposed sliding mode control schemes by using the estimated state variables are compared with the results of proposed sliding control schemes by using real state variables. Figures 8 and 9 obviously depict the prompt convergence of the second order sliding mode controllers in comparison with traditional sliding mode controllers for both short and long amplitude of desired output. In addition, it is obvious that the second order sliding mode controllers can totally remove the chattering effect.

Figure 10 displays the closed-loop response, applied voltage, phase plane and sliding surface for short displacement ($5\mu m$) of the actuator utilizing the

time-varying second order sliding mode control. Then, to compare the robust performance of the proposed method with that of the SOSMC, the uncertain model dynamics is simulated as:

$$\ddot{x} = \frac{1}{2.35 \times 10^{-9}} [-(0.0363x + 4.5 \times 10^{-3})\dot{x} - 0.6x + 1.9 \times 10^{-8}V^2 + \xi(t, x, \dot{x}, V)] \quad (42)$$

where $\alpha = 100$ is considered as an uncertain parameter. Figures 11 and 12 show the position and velocity error, respectively, in the presence of a parameter uncertainty. As can be seen from Figs.11 and 12, the traditional second order sliding mode control (SOSMC) is not robust enough in the contrary to the proposed time-varying second order sliding mode control (TVSOSMC) with respect to the parameter uncertainty. However, the proposed TVSOSMC could successfully enhance the robust performance over time.

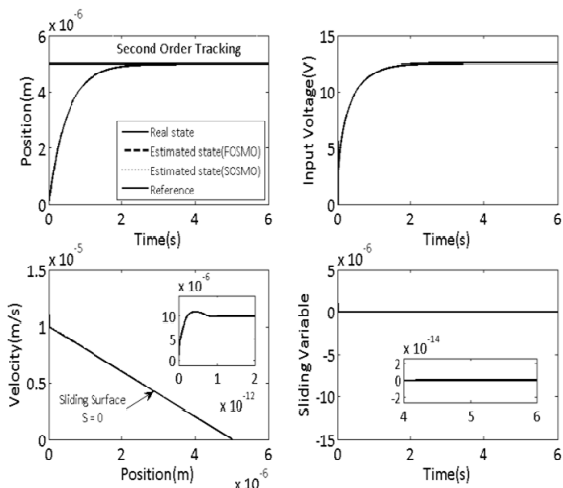


Figure 8. Position, Control input, Phase plane, and Sliding variable of the system for a short desired position $x_d = 5 \mu m$ by using SOSMC

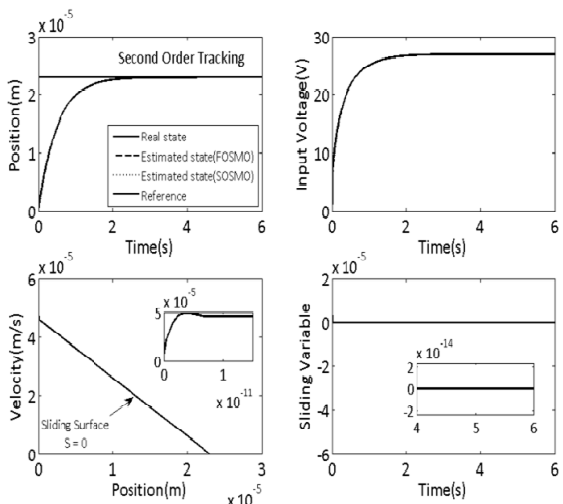


Figure 9. Position, Control input, Phase plane, and Sliding variable of the system for a long desired position $x_d = 23 \mu m$ by using SOSMC

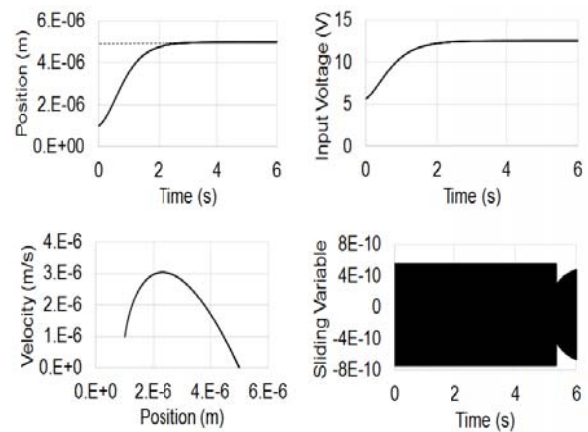


Figure 10. Position, Control input, Phase plane, and Sliding variable of the system for a short desired position $x_d = 5 \mu m$ by using TVSOSMC

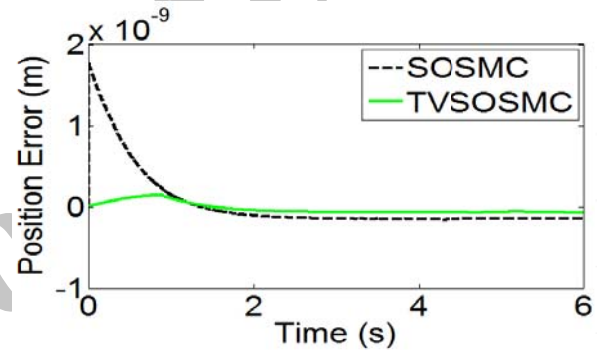


Figure 11. Position error based on the traditional second order sliding mode control (SOSMC) and the proposed time-varying second order sliding mode control (TVSOSMC) w.r.t uncertainty

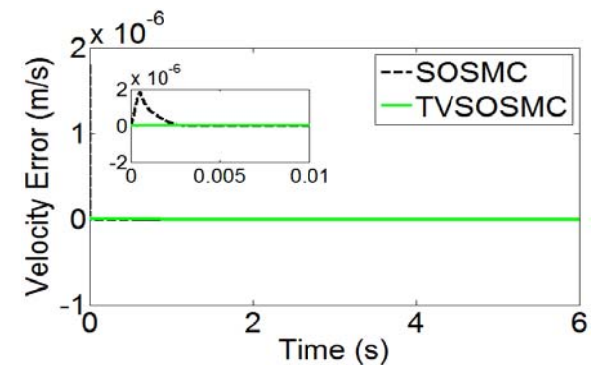


Figure 12. Velocity error based on the traditional second order sliding mode control (SOSMC) and the proposed time-varying second order sliding mode control (TVSOSMC) w.r.t uncertainty

Conclusion

Two nonlinear observers based on the sliding mode concept are proposed in this study, i.e. traditional first order sliding mode observer (FOSMO) and second order sliding mode observer (SOSMO), in order to estimate the state variables of a MEMS optical switch

with nonlinear terms and disturbances. Robustness and stability of the proposed FOSMO is proved by Lyapunov second method and SOSMO is designed based on the super-twisting algorithm. Moreover, the effectiveness of SOSMO in eliminating the effect of chattering is demonstrated through simulations. Sliding mode control laws are then designed by using the estimated state variables from the proposed observers to improve the dynamic closed-loop performance of the MEMS optical switch. As a result, second order sliding mode control law is an efficient control scheme which is capable of totally removing the chattering effect resulted by high frequency switching in the conventional sliding mode control. Next, to enhance the robust performance of the designed second order sliding mode control, new time-varying sliding surface algorithms based on shifting and/or rotating the sliding variables are employed. Finally, the simulation results indicate that the observer states converge to the actual states very quickly in the presence of disturbances. Also, tracking of the desired position with short and long amplitudes is accomplished within the specified limitation for the control input.

References

- Chen, R.T., Nguyen, H. and Wu, M.C., "A high-speed low-voltage stress-induced micromachined 2×2 optical switch," *IEEE Photonics Technology Letters*, Vol. 11, No. 11, 1999, pp. 1396-1398.
- Giles, C.R., Aksyuk, V., Barber, B., Ruel, R., Stulz, L., and Bishop, D., "A silicon MEMS optical switch attenuator and its use in light wave subsystems," *IEEE Journal of Selected Topics in Quantum Electronics*, Vol. 5, No. 1, 1999, pp. 18-25.
- Owusu, K.O., Lewis, F.L., Borovic, B., and Liu, A.Q., "Nonlinear control of a MEMS optical switch," *45th IEEE Conf. Decision and Control*, San Diego, CA, 2006, pp. 597-602.
- Ebrahimi, B., and Bahrami, M., "Robust sliding-mode control of a MEMS optical switch," *Journal of Physics: Conference Series*, Vol. 34, 2006, pp. 728-733.
- Torabi, Z.K., Vali, M., Ebrahimi, B., and Bahrami, M., "Robust control of nonlinear MEMS optical switch based on quantitative feedback theory," *5th IEEE Int. Conf. on Nano/Micro Engineered and Molecular Systems (NEMS)*, Xiamen, China, 2010, pp. 122-128.
- Barbot, J.P., Djemai, M., and Boukhobza, T., "Sliding Mode Observers," *Sliding Mode control in Engineering*, Chap. 4, edited by W. Perruquetti and J.P. Barbot, Marcel Dekker, New York, 2002.
- Xiong, Y., and Saif, M., "Sliding mode observer for nonlinear uncertain systems," *IEEE Transaction on Automatic control*, Vol. 46, No. 12, 2001, pp. 2012-2017.
- Davila, J., Fridman, L., and Levant, A., "Second-order sliding-mode observer for mechanical systems," *IEEE Transaction on Automatic control*, Vol. 50, No. 11, 2005, pp. 1785-1789.
- Slotine, J.J., and Li, W., *Applied Nonlinear Control*, Prentice Hall, New Jersey, 1991.
- Levant, A., "Sliding order and sliding accuracy in sliding mode control," *International Journal of Control*, Vol. 58, No. 6, 1993, pp. 1247-1263.
- Bartolini, G., Ferrara, A., and Usai, E., "Output tracking control of uncertain nonlinear second-order systems," *Automatica*, Vol. 33, No. 12, 1997, pp. 2203-2212.
- Choi, S.-B., Park, D.-W., and Jayasuriya, S., "A time-varying sliding surface for fast and robust tracking control of second-order uncertain systems," *Automatica*, Vol. 30, No. 5, 1994, pp. 899-904.
- Bartoszewicz, A., "A comment on a time-varying sliding surface for fast and robust tracking control of second-order uncertain systems," *Automatica*, Vol. 31, No. 12, 1995, pp. 1893-1895.
- Yongqiang, J., Xiangdong, L., Wei, Q., and Chaozhen, H., "Time-varying sliding mode controls in rigid spacecraft attitude tracking," *Chinese Journal of Aeronautics*, Vol. 21, pp. 352-360 (2008).
- Li, J., Zhang, Q.X., and Liu, A.Q., "Advanced fiber optical switches using deep RIE (DRIE) fabrication," *Sensors and Actuators A: Physical*, Vol. 102, No. 3, 2003, pp. 286-295.
- Senturia, S.D., *Microsystem Design*, Springer, New York, USA, 2001.
- Liu, A.Q., Zhang, X.M., Lu, C., Wang, F., Lu, C., and Liu, Z.S., "Optical and mechanical models for a variable optical attenuator using a micromirror drawbridge," *J. Micromech. Microeng.*, Vol. 13, No. 3, 2003, pp. 400-411.
- Borovic, B., Hong, C., Liu, A.Q., Xie, L., and Lewis, F.L., "Control of a MEMS optical switch," *43rd IEEE Conf. Decision and Control*, Vol. 3, Paradise Islands, The Bahamas, 2004, pp. 3039-3044.